General Relativity and Gravitation (2022) 54:5
https://doi.org/10.1007/s10714-021-02886-0

RESEARCH ARTICLE

Reentrant phase transition with a single critical point of the Hayward-AdS black hole

Yi-Peng Liu[1] · Hui-Ming Cao[1] · Wei Xu[1]

Received: 1 November 2021 / Accepted: 29 November 2021 / Published online: 10 January 2022

Abstract

The reentrant phase transition (RPT) is composed of at least two phase transition, which has previously been observed in the Condensed Matter Theory/systems, and now has been found with a renewal interest in black hole thermodynamics. For the RPT, there exist always two and several critical points; while the first order phase transition always corresponds to a single critical point. In this paper, we present a black hole thermodynamical systems with a single critical point possessing the RPT, other than a first order phase transition. Concretely, we focus on the Hayward-AdS black hole, i.e. the AdS black hole in the gravity with a nonlinear electrodynamics, consider its extended thermodynamics, and investigate its critical phenomena and phase structure, especially the RPT in detail. The number of critical points and the types of phase transition depend on the strength constant of the nonlinear electromagnetic field. We introduce an unexpected RPT with a single physical critical point for the first time. We also present all distinct and physical critical RPT points in the phase diagrams.

Keywords Reentrant phase transition · Critical point · Hayward-AdS black hole

Contents

✉ Wei Xu
xuwei@cug.edu.cn

Yi-Peng Liu
20141002685@cug.edu.cn

Hui-Ming Cao
1014383185@qq.com

[1] School of Mathematics and Physics, China University of Geosciences, Wuhan 430074, China

1 Introduction

Black hole thermodynamics is one of great importance subjects in gravitational theory, since it could provide a further insight into the understanding of quantum theories of gravity. Actually, black holes can always behave like an ordinary thermodynamical systems and undergo the phase transition, which is a most remarkable property in black hole thermodynamics and can relate a gravitational system to an accessible experimental system. The pioneering work on black holes phase transition was done by Hawking and Page, who proved that a first order phase transition occurs between a large AdS black hole and a thermal AdS vacuum [1]. Especially, this so-called Hawking-Page phase transition could be explained as the confinement/deconfinement phase transition of gauge field [2], inspired by the AdS/CFT correspondence [3–5]. These open a grand window to explore the holographic and quantum understanding of critical phenomena and phase transition in general AdS spacetime. Later, it has been claimed that the first order phase transition of RN-AdS black hole [6,7] is similar to the liquid/gas phase transition of the van der Waals fluid. After treating the cosmological constant as a thermodynamic pressure and its conjugate quantity as thermodynamic volume [8–13], the SBH/LBH phase transition of RN-AdS black hole is established [14], which is precisely analogous to the liquid/gas phase transition of the van der Waals fluid (See also [15,16] for reviews). More complicated phase structure also emerge in black hole thermodynamics, including the RPT [17,18] and superfluid phase transition [19].

The RPT is composed of at least two phase transition, which has previously been observed in a nicotine/water mixture [20], granular superconductors, liquid crystals, binary gases, ferroelectrics and gels (see [21] and the references therein). Recently, it revealed that there exist a RPT between the IBH/SBH/LBH in AdS spacetime [17,18]. This RPT is accompanied by a finite jump in the Gibbs free energy, which referred to a zeroth-order phase transition that has been observed in superfluidity and superconductivity [22]. The study were also generalized to various setups [23–32]. Furthermore, microscopic origin of the RPTs for AdS black holes has been explored in [33], which is closely related to a quantum statistical systems. These may shed some lights on the microcosmic and quantum understanding of black hole thermodynamics and phase transition.

It is interesting to consider the relationship between RPT and the number of critical points. No matter in classical thermodynamical systems (e.g. van der Waals gas), or in quantum thermodynamical systems (e.g. black hole), the relationship between phase transition and the number of critical points is subtle. It is well known that a first order phase transition always corresponds to a single critical point (e.g. SBH/LBH phase transition of AdS black hole [14]); a second order phase transition always

corresponds to infinity critical points (e.g. superfluid phase transition of AdS black hole [19]); while for RPT, there are always two and several critical points. It is worth noting that in all references mentioned above, the RPTs of AdS black holes correspond to two and several physical critical points. However, we get that a thermodynamical systems with a single critical point can possess RPT, other than a first order phase transition. Concretely, we take the Hayward-AdS black hole, i.e. the AdS black hole in the gravity with a nonlinear electrodynamics as an example and we investigate its critical phenomena and phase structure in detail.

The interest for nonlinear electrodynamics has started with the precursor work of Born and Infeld, in order to modify the standard Maxwell theory and eliminate the problem of infinite energy of the electron [34]. Recent, the nonlinear electrodynamics have been proved to be excellent laboratories in order to circumvent some problems that occur in the standard Maxwell theory. Indeed, the nonlinear electrodynamics theory can emerge naturally in the context of low-energy limit of heterotic string theory [35]. Due to the fact that the nonlinear electrodynamics theory is a powerful tool for the construction of regular black hole solutions [36,37], it becomes more popular and attracts a great attentions (e.g. [38–50]). Actually, the black hole with a nonlinear electrodynamics presented in this paper, i.e. the Hayward-AdS black hole, can reduce to the famous Hayward black hole, which is just a regular black hole solution. Besides, the thermodynamics properties of the gravity with a nonlinear electrodynamics is also an active research area in the current literature (e.g. [51–60].) For example, the Born-Infeld AdS black hole has a SBH/LBH phase transition and a RPT between the IBH/SBH/LBH due to the different strength of the nonlinear electrodynamics [17]. These property render more attractive the studies of the gravity with a nonlinear electrodynamics. For the Hayward-AdS black hole case studied in this paper, it also has a complicated phase structure. Especially, an unexpected RPT will be presented for the first time, which only corresponds to a single physical critical point; while usually the RPT should correspond to two physical critical points. The whole phase structure of the Hayward-AdS black hole is also discussed. The number of critical points and the types of phase transition depend on the constant of the nonlinear electromagnetic field, i.e. the strength of the nonlinear electrodynamics. Moreover, we present the way obtaining the critical RPT points (T_z, P_z) and (T_t, P_t), and give their exact values. Especially for the unexpected RPT, P_z may be negative and physically unacceptable; hence we also derive the physical critical RPT point $(T_0, 0)$.

The paper is organized as follows. We will firstly revisit the Hayward-AdS black hole and its extended thermodynamics in next sections. In Sects. 3 and 4, we study the critical behavior and phase transition, respectively. Finally some concluding remarks are given in Sect. 5.

2 The black hole system and its extended thermodynamics

We firstly revisit the Hayward-AdS black hole, which is a general two-parameters family black hole solution in the gravity with a nonlinear electrodynamics [39]

$$ds^2 = -f(r)dt^2 + \frac{dr^2}{f(r)} + r^2\left(d\theta^2 + \sin^2\theta d\phi\right), \tag{1}$$

$$f(r) = 1 - \frac{2M_{eff}}{r} - \frac{2q^3r^2}{\alpha(r^3+q^3)} + \frac{r^2}{\ell^2}, \quad A = Q_m \cos\theta d\phi, \tag{2}$$

where $\Lambda = -\frac{3}{\ell^2}$ is the cosmological constant the constant $\alpha > 0$ characterizes the strength of the nonlinear electrodynamics field and has the dimension of length squared. q is the parameter related to the magnetic charge of the Hayward-AdS black hole

$$Q_m = \frac{q^2}{\sqrt{2\alpha}}. \tag{3}$$

The AMD mass of the Hayward-AdS black hole is

$$M_{ADM} = M_{eff} + \frac{q^3}{\alpha}, \tag{4}$$

which can be read off from the behavior of the metric function at asymptotic infinity

$$f(r) = \frac{r^2}{\ell^2} + 1 + \frac{2(M_{eff} + q^3/\alpha)}{r} + \mathcal{O}(\frac{1}{r^4}).$$

As in the neutral limit, the solution reduces to the Schwarzschild AdS black hole, one can refer to M_{eff} as the Schwarzschild mass. Besides, for any non-vanishing M_{eff}, the above black hole solution behaves singular at the origin, which could never be unavoidable. When M_{eff} is vanishing, the solution reduces to the Hayward black hole [38,39], which is a famous regular black hole, since its curvature polynomials R, $R_{\mu\nu}R^{\mu\nu}$, $R_{\mu\nu\rho\sigma}R^{\mu\nu\rho\sigma}$ all have a regular limit at the origin. The critical phenomena of the Hayward black hole was study in detail in [39], and a liquid/gas phase transition was found.

Other thermodynamical quantities are also presented in [39]. The black hole temperature, entropy and electric potential are

$$T = \frac{1}{4\pi\, r_+} - \frac{3q^6 r_+}{2\pi\alpha(q^3+r_+^3)^2} + \frac{3r_+}{4\pi\ell^2},$$
$$S = \pi\, r_+^2, \quad \Phi = \frac{3q^4(2r_+^3+q^3)}{\sqrt{2\alpha}(r_+^3+q^3)^2}, \tag{5}$$

respectively, where r_+ is the radius of the event horizon. In the following paper, we will discuss thermodynamics in the extended phase space, where the cosmological constant is treated as a thermodynamic variable, i.e.

$$P = -\frac{\Lambda}{8\pi} = \frac{3}{8\pi\ell^2}, \tag{6}$$

with the conjugated thermodynamic volume being $V = \frac{\partial M_{ADM}}{\partial P}|_{(S,Q_m,\alpha)} = \frac{4\pi r_+^3}{3}$. Then it is easy to check the first law of thermodynamics

$$\mathrm{d}M_{ADM} = T\mathrm{d}S + \Phi \mathrm{d}Q_m + V\mathrm{d}P + \Pi \mathrm{d}\alpha, \tag{7}$$

where $\Pi = \frac{\partial M_{ADM}}{\partial \alpha}|_{(S,Q_m,P)} = \frac{q^6(2r_+^3-q^3)}{4\alpha^2(r_+^3+q^3)^2}$ conjugates to α. Besides, the Smarr relation becomes

$$M_{ADM} = 2TS + \Phi\, Q_m - 2PV + 2\alpha\Pi, \tag{8}$$

which is perfectly consistent with the scaling dimensional argument. Finally, in order to observe the global thermodynamic stability, we introduce the Gibbs free energy

$$G = M_{ADM} - TS = \frac{r_+}{3} - \frac{1}{3}\pi r_+^2 T + \frac{q^6}{\alpha(q^3+r_+^3)} + \frac{q^6 r_+^3}{\alpha(q^3+r_+^3)^2}. \tag{9}$$

3 Critical behavior

3.1 Equation of state and critical points

We firstly calculate the critical points of the system. Based on the temperature Eq. (5), we can directly derive the equation of state

$$P = \frac{T}{2r_+} - \frac{1}{8\pi r_+^2} + \frac{3q^6}{4\pi\alpha(r_+^3+q^3)^2}. \tag{10}$$

Comparing with the van der Waals fluid equation, it is easy to find the specific volume $v = 2r_+$. Therefore we will choose the horizon radius r_+ as the thermodynamical variable in the equation of state for the black hole system hereafter in this paper, instead of the specific volume v.

Always the critical point occurs when P has an inflection point, i.e.

$$\frac{\partial P}{\partial r_+}|_{(T=T_c,r_+=r_c)} = \frac{\partial^2 P}{\partial r_+^2}|_{(T=T_c,r_+=r_c)} = 0, \tag{11}$$

where the subscript c stands for the quantities at the critical point. We can obtain the critical pressure and temperature

$$P_c = \frac{1}{8\pi r_+^2} + \frac{3q^6(q^3-5r_+^3)}{\alpha\pi(q^3+r_+^3)^3}, \tag{12}$$

$$T_c = \frac{1}{2\pi r_+} + \frac{9q^6 r_+^4}{\alpha\pi(q^3+r_+^3)^3} \tag{13}$$

with the critical horizon radius r_c which is the root of the equation

$$\alpha(q^3 + r_+^3)^4 + 18q^6 r_+^5(4q^3 - 5r_+^3) = 0. \tag{14}$$

In order to explore the critical points, we would like to introduce some reduced thermodynamical quantities. We first list the length dimensions of the relevant parameters and thermodynamic quantities:

$$\ell = [L], \quad q = [L], \quad \alpha = [L]^2, \quad P = [L]^{-2}, \quad T = [L]^{-1}, \tag{15}$$

therefor we can choose the reduced thermodynamical quantities for the critical point and the reduced constant of the electromagnetic field as

$$P_c = \frac{p_c}{8\pi r_c^2}, \quad T_c = \frac{t_c}{2\pi r_c}, \quad r_c = Rq, \quad \alpha = \gamma q^2. \tag{16}$$

Now we can simplify the critical points as

$$p_c = \frac{60R^2(R^3 - R_P^3)(R^3 - R_{P1}^3)}{\gamma(R^3+1)^4}, \quad t_c = \frac{72R^5(R^3 - R_T^3)}{\gamma(R^3+1)^4}, \quad R_T = \frac{10^{1/3}}{2} \approx 1.08, \tag{17}$$

$$R_P = \frac{(800 + 300\sqrt{6})^{1/3}}{10} \approx 1.15, \quad R_{P1} = \frac{(800 - 300\sqrt{6})^{1/3}}{10} \approx 0.40, \tag{18}$$

where the equation for the critical horizon radius is

$$\gamma = \gamma(R) = \frac{18R^5(5R^3 - 4)}{(R^3+1)^4}. \tag{19}$$

For positive pressure p, we find a constraint $0 < R < R_{P1}$ or $R > R_P$; while positive temperature τ leads to

$$R > R_T. \tag{20}$$

To sum up, we find that the physical critical points with positive temperature and pressure require

$$R > R_P. \tag{21}$$

Since we focus on the physical critical points, we plot the curve of $\gamma - R$ in Fig. 1. It is easy to observe that there exist some special values of γ: γ_m corresponds to the maxima of $\gamma(R)$; γ_P and γ_T denote the states with vanishing critical pressure and temperature, respectively. Then the discussion about the number of the physical critical points could be divided into the following subcases:

- When $\gamma > \gamma_m$, there exists no value of R, namely one can never find a critical horizon radius, hence there is no critical point;

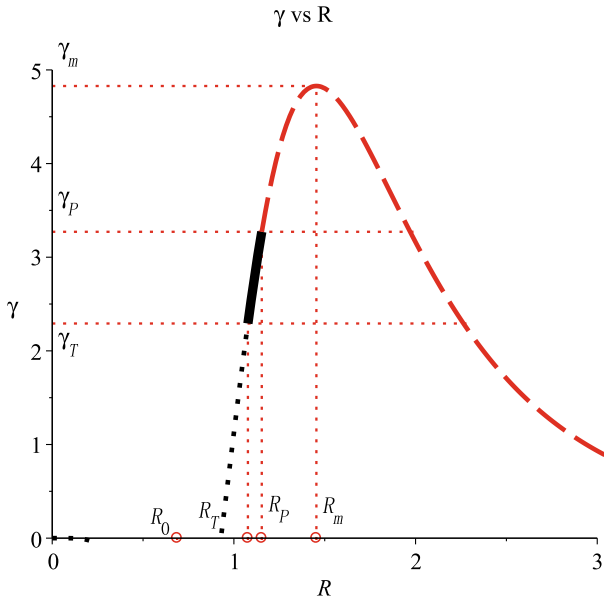

Fig. 1 Curve of $\gamma - R$, which characterizes different cases for the physical critical points. The (red) dashed line denotes the physical critical points with positive temperature and pressure, while the (black) solid line corresponds to the critical points with positive temperature and negative pressure, and the (black) dotted one corresponds to the critical points with negative temperature and pressure (colour figure online)

- When $\gamma = \gamma_m$, the case corresponds to a double critical horizon radius $R = R_m$. As $R_m > R_P > R_T$, the critical pressure and temperature both are positive, there exists a single critical points. Since

$$\frac{\partial \gamma(R)}{\partial R} = -\frac{360R^4(R^3 - R_m^3)(R^3 - R_0^3)}{(R^3+1)^5}, \tag{22}$$

$$R_m = \frac{(1700 + 300\sqrt{21})^{1/3}}{10} \approx 1.45, \quad R_0 = \frac{(1700 - 300\sqrt{21})^{1/3}}{10} \approx 0.69, \tag{23}$$

  we can get $\gamma_m = \gamma(R)|_{R=R_m} = \frac{1000}{9(1700+300\sqrt{21})^{1/3}(\sqrt{21}-3)} \approx 4.83$.
- When $\gamma_P < \gamma < \gamma_m$, each γ corresponds to two critical horizon radius R with positive pressure and temperature, therefore one can find two physical critical points;
- When $\gamma_T < \gamma \leq \gamma_P$, there is a single physical critical point, while another corresponds to zero or negative pressure and positive temperature. We can obtain $\gamma_P = \gamma(R)|_{R=R_P} = \frac{1000}{9(800+300\sqrt{6})^{1/3}(11\sqrt{6}-24)} \approx 3.27$.
- When $\gamma \leq \gamma_T$, there also exists a single critical horizon radius; while another corresponds to negative pressure and temperature (or zero), thus physically unacceptable. Here we can get $\gamma_T = \gamma(R)|_{R=R_T} = \frac{40}{81}10^{2/3} \approx 2.29$.

Table 1 The behaviors of critical points for different values of γ (or α). The values of special γ are $\gamma_m \approx 4.83$, $\gamma_P \approx 3.27$, $\gamma_T \approx 2.29$

γ	$\gamma \leq \gamma_T$	$\gamma_T < \gamma \leq \gamma_P$	$\gamma_P < \gamma < \gamma_m$	$\gamma = \gamma_m$	$\gamma > \gamma_m$
Number of critical points	1	1	2	1	0

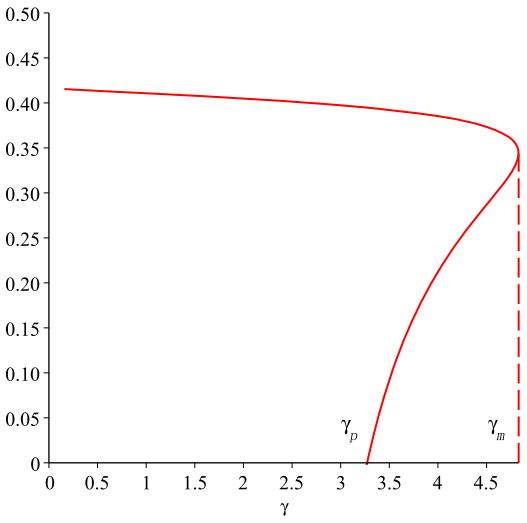

Fig. 2 $\frac{P_c v_c}{T_c}$ vs γ. The two-values part of curve denotes the cases with two physical critical points

We summarize the critical points for different γ in the Table 1. On the other hand, we can calculate the interesting relation $\frac{P_c v_c}{T_c}$, which is a universal constant for different γ as shown in Fig. 2. The constants are slightly different from the value $\frac{3}{8}$ of the van der Waals fluid. The curves of $\frac{P_c v_c}{T_c} - \gamma$ could be divided into two branches: the above branch decreases as γ increases, while γ enlarges the constant $\frac{P_c v_c}{T_c}$ in the below one. When $R \to +\infty$, then $\gamma \to 0$, and the constant $\frac{P_c v_c}{T_c}$ reaches the maxima $\frac{5}{12}$.

3.2 Critical exponents and coexistence states

Here we would like to explore the critical exponents and coexistence states, which will be useful of the discussion about the complicated phase structure.

For $\gamma \leq \gamma_m$, there always exist critical points, we firstly calculate the critical exponents. We still follow the transformation Eq. (16) and define the following dimensionless thermodynamical variables

$$\Theta = \frac{P}{P_c}, \quad \omega = \frac{T}{T_c} - 1, \quad \phi = \frac{r}{r_c} - 1. \tag{24}$$

Then we can obtain the dimensionless equation of state, which has a complicated form and we do not list here. After taking a Taylor expansion, and using the relation Eq. (19), we can derive

$$\Theta = 1 - a\omega(\phi - 1) - b\phi^3 + \mathcal{O}(\omega\phi^2, \phi^4), \tag{25}$$

where $a = \frac{12R^3(R^3-R_T^3)}{5(R^3-R_P^3)(R^3-R_{P1}^3)}$, $b = \frac{2R^3(R^3-R_m^3)(R^3-R_0^3)}{(R^3+1)(R^3-R_P^3)(R^3-R_{P1}^3)}$. It is clear from Eq. (25) that the critical exponents are

$$\alpha = 0, \quad \beta = \frac{1}{2}, \quad \gamma = 1, \quad \delta = 3, \tag{26}$$

which govern the behaviour of the specific heat at constant volume $C_V \propto |\omega|^{-\alpha}$, the order parameter $\phi \propto |\omega|^{\beta}$, the susceptibility/compressibility $\frac{\partial\phi}{\partial\Theta}|_\omega \propto |\omega|^{-\gamma}$ and the ordering field $\Theta \propto |\phi|^{\delta}$ near a critical point, respectively.

Now we using Maxwell's equal area law to study the coexistence states for the first order phase transition. From Eq. (25), one can obtain the following equation

$$0 = \int_{\phi_1}^{\phi_2} \phi \frac{\mathrm{d}\Theta}{\mathrm{d}\phi}\mathrm{d}\phi \Rightarrow \frac{3}{4}b(\phi_1^4 - \phi_2^4) + \frac{1}{2}a\omega(\phi_1^2 - \phi_2^2) = 0, \tag{27}$$

where the subscripts 1 and 2 stand for the LBH and SBH phases, respectively. On the other hand, the physical phase equilibrium condition (i.e. the isobar pressure condition) gives

$$\Theta|_{\phi_1} = \Theta|_{\phi_2} \Rightarrow a\omega(\phi_1 - \phi_2) + b(\phi_1^3 - \phi_2^3) = 0. \tag{28}$$

Equations (27) and (28) together give a unique non-trivial solution ($\phi_1 \neq \phi_2$)

$$\phi_{1,2} = \pm\sqrt{-\frac{a}{b}\omega}, \tag{29}$$

where

$$\frac{a}{b} = \frac{6(R^3 - R_T^3)(R^3 + 1)}{5(R^3 - R_m^3)(R^3 - R_0^3)}. \tag{30}$$

Then when $a/b < 0$, we conclude that the coexistence of smaller and larger black hole phases requires $\omega > 0$; in other words, only when $T > T_c$ can the two stable black hole phases exist at the same pressure. Conversely, if $a/b > 0$, the phase transition will occur when $T < T_c$. Noting that the coexistence states depend on the relationship between R and R_m, R_T (since all R ar bigger that R_0).

4 Phase structure

4.1 No phase transition when $\gamma \geq \gamma_m$

When $\gamma > \gamma_m$, there is no critical point. The curves of $P - r_+$ and $G - P$ are depicted in Fig. 3, where one can not find the $P - r_+$ oscillatory behavior and the

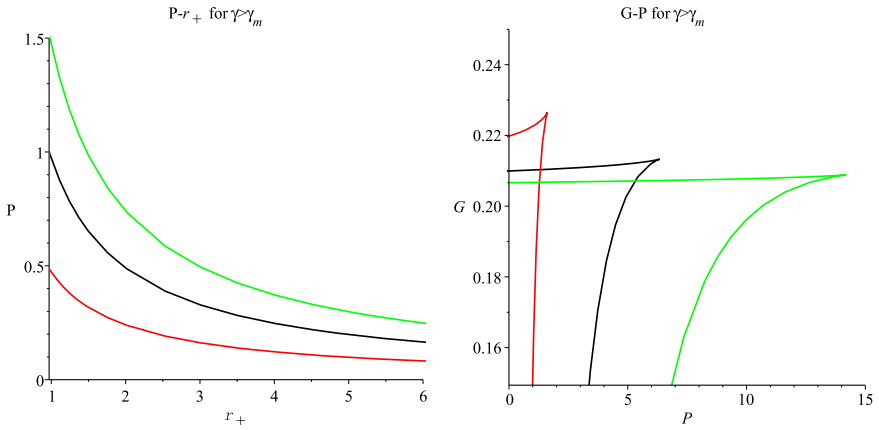

Fig. 3 Curves of $P - r_+$ and $G - P$ for the cases with $\gamma > \gamma_m$. There exists no critical phenomena and phase transition. In both plots, the temperature of isotherms increase from left to right

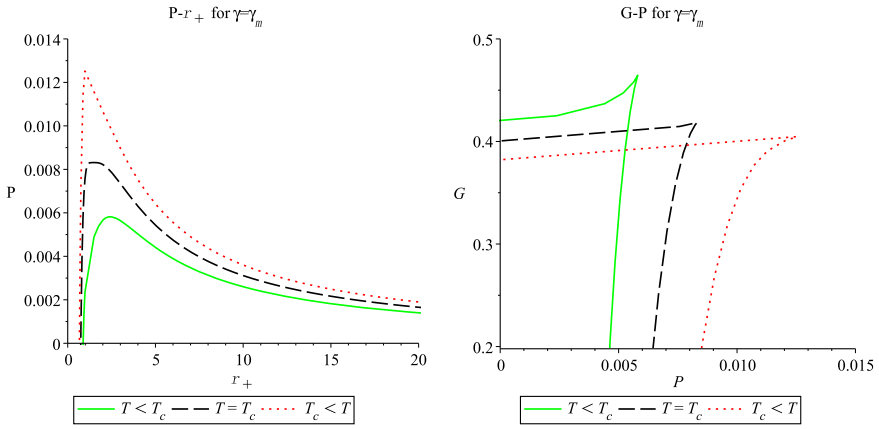

Fig. 4 Curves of $P - r_+$ and $G - P$ for the case with $\gamma = \gamma_m$. There exists no critical phenomena and phase transition. In left plot, the temperature of isotherms decrease from left to right, while they increase from left to right in the right plot

classical "swallow tail". Therefore, one can never find the critical phenomena and phase transition.

When $\gamma = \gamma_m$, the situation becomes interesting, as there exists a double critical horizon radius $R = R_m$. We plot the diagrams of $P - r_+$ and $G - P$ in Fig. 4, and there exists no $P - r_+$ oscillatory behavior and the classical "swallow tail" as well. Thus, there is no critical phenomena and phase transition, even this case of the system possess a critical point. One can understand the unexpected phenomena by explore the coexistence states. From Eq. (30), one can find $\frac{a}{b}$ diverges when $R = R_m$ (i.e. $\gamma = \gamma_m$). As a result, there exists no coexistence state as $\phi_1 = \phi_2 \to \infty$. The double

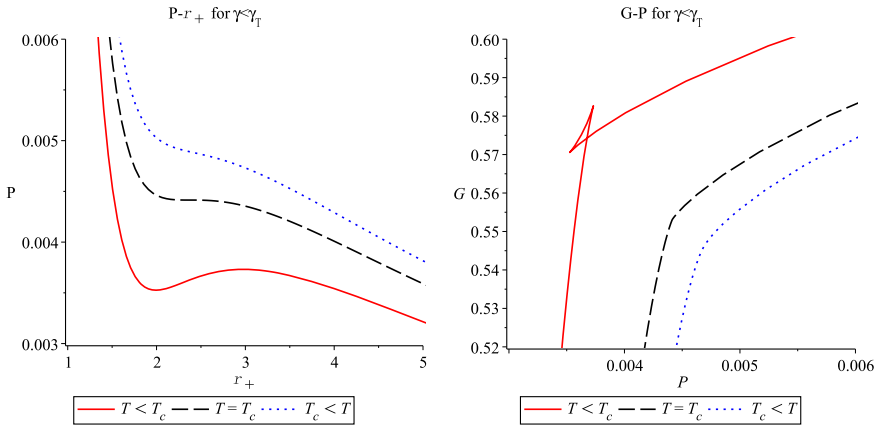

Fig. 5 Curves of $P - r_+$ and $G - P$ for the cases with $\gamma \leq \gamma_T$. There are the $P - r_+$ oscillatory behavior and the classical "swallow tail" characterizing the SBH/LBH phase transition. In both plots, the temperature of isotherms increase from left to right

critical point ($p = p_c, t = t_c, R = R_m$) could not characterize the existence of a first order SBH/LBH phase transition.

4.2 First order SBH/LBH phase transition when $\gamma \leq \gamma_T$

When $\gamma \leq \gamma_T$, there is a single physical critical point, while another positive critical horizon radius corresponds to negative pressure and negative/zero temperature, thus physically unacceptable. As shown in Fig. 5, one can find the $P - r_+$ oscillatory behavior and the classical "swallow tail" characterizing the SBH/LBH phase transition when $T < T_c$, which is denoted as the (red) solid line. This is consistent with the discussion about the coexistence states in the last section. Actually, from Fig. 1, we can obtain that the physical critical horizon radius has the relationship $R > R_m > R_T > R_0$ when $\gamma \leq \gamma_T$. Considering this relationship and Eq. (30) together, we can find $\frac{a}{b} > 0$, which leads to $\omega < 0$ and indicates the first order phase transition occurring when $T < T_c$.

4.3 RPT when $\gamma_P < \gamma < \gamma_m$

When $\gamma_P < \gamma < \gamma_m$, there is two physical critical points which always indicates the existence of a RPT. The behavior of pressure P and Gibbs free energy G are depicted in Fig. 6. For the isotherms with temperature $T_{c1} < T < T_{c2}$ which is denoted as the (gold) solid line, we can observe two $P - r_+$ oscillatory behavior and multi-characteristic "swallow tail" behavior characterizing the possible phase transition. We can study the coexistence states to confirm this result. When $\gamma_P < \gamma < \gamma_m$, we can find the relationship of two physical critical horizon radius from Fig. 1, i.e. $R_1 > R_m > R_2 > R_P > R_T > R_0$. Then Eq. (30) leads to $\frac{a}{b} > 0$ near the critical

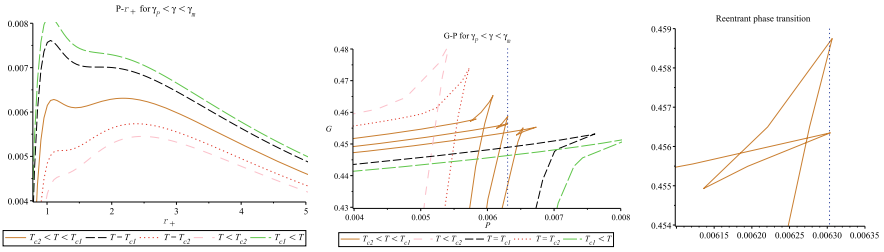

Fig. 6 Curves of $P - r_+$ and $G - P$ for the cases with $\gamma_P < \gamma < \gamma_m$. There exists a RPT. In $P - r_+$ plot, the temperature of isotherms decrease from left to right, while they increase from left to right in $G - P$ plot

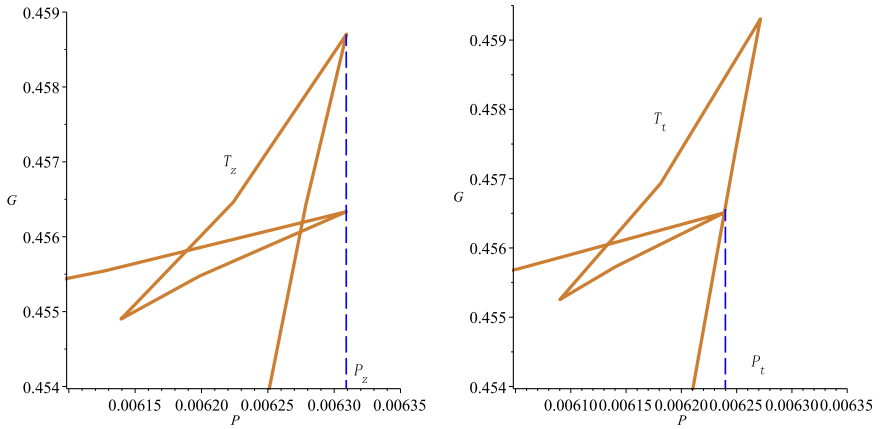

Fig. 7 Characteristic behavior of RPT

point (R_1, T_{c1}, P_{c1}) implying that the phase transition will occur when $T < T_{c1}$; while near another critical point (R_2, T_{c2}, P_{c2}), it is $\frac{a}{b} < 0$ and the phase transition will occur when $T > T_{c2}$; ultimately, a phase transition (at least two "swallow tail") should occur when $T_{c2} < T < T_{c1}$.

Considering the phase transition when $T_{c2} < T < T_{c1}$, it is the first order SBH/LBH phase transition occurring for $T < T_{c1}$ and terminating at $T = T_t$. Especially, there exists a certain range of temperatures $T \in (T_t, T_z)$, where the global minimum of Gibbs free energy G is discontinuous as shown in the right one of Fig. 6. This results in the so-called "zeroth-order phase transition", for which two separate branches of IBH and SBH coexist and meanwhile are separated by a finite jump in G. In this range of temperatures, the first order SBH/LBH phase transition and the "zeroth-order phase transition" between the IBH and SBH both appear, which just corresponds to the RPT.

One can denote (T_t, P_t) and (T_z, P_z) as the critical RPT points, which are difficult to obtain analytically. Here we present the way to calculate their values, so that one can obtain the exact critical RPT points by the numerical method. The cases for the critical RPT points are depicted in Fig. 7. From the left one in Fig. 7, we see that at the critical RPT point (T_z, P_z), the two extremal points of $\frac{\partial P}{\partial r_+} = 0$ have the same value of

Table 2 The critical points and the critical RPT points in triple phase diagram when $\gamma_p < \gamma < \gamma_m$

γ	(τ_{c2}, p_{c2})	(τ_{c1}, p_{c1})	(τ_z, p_z)	(τ_t, p_t)
4.8	(0.439785, 0.207235)	(0.439962, 0.207478)	(0.439867, 0.207352)	(0.439517, 0.206846)
4.5	(0.419590, 0.184261)	(0.427108, 0.194600)	(0.423349, 0.190314)	(0.422695, 0.189239)
4	(0.373121, 0.128990)	(0.407473, 0.176242)	(0.390323, 0.159300)	(0.388315, 0.155643)
3.5	(0.307386, 0.048211)	(0.388256, 0.159438)	(0.348077, 0.124851)	(0.344906, 0.118613)
10/3	(0.279898, 0.013885)	(0.381787, 0.154012)	(0.331299, 0.112656)	(0.327836, 0.105684)

P, i.e. P_z. From the right one in Fig. 7, we find that at the critical RPT point (T_t, P_t), one extremal point of $\frac{\partial P}{\partial r_+} = 0$ has the same value of P (i.e. P_t) and G with a SBH (which we denote its thermodynamical quantities as (r_c, T_c, P_c)). After introducing the transformation

$$P = \frac{p}{8\pi q^2}, \quad T = \frac{\tau}{2\pi q}, \quad r_+ = Rq, \quad \alpha = \gamma q^2, \tag{31}$$

we can obtain the equations for (τ_z, p_z) and (τ_t, p_t), namely,

$$\frac{\partial p}{\partial R}|_{(\tau=\tau_z, R=R_a)} = \frac{\partial p}{\partial R}|_{(\tau=\tau_z, R=R_b)} = 0, \quad p_z = p_a = p_b, \tag{32}$$

and

$$\frac{\partial p}{\partial R}|_{(\tau=\tau_t, R=R_a)} = 0, \quad p_t = p_a = p_c, \quad G_t = G_a = G_c. \tag{33}$$

respectively. Finding out this point, we can derive the values of the critical RPT points (τ_t, p_t) and (τ_z, p_z). We present these points for $\gamma_p < \gamma < \gamma_m$ together with the critical point $(\tau_{c1,c2}, p_{c1,c2})$ in Table 2.

Finally, this novel RPT can be also clearly illustrated in the $p - \tau$ diagrams (i.e. $P - T$ diagrams) as shown in Fig. 8. There exists a SBH/LBH line of coexistence states, which ends in a critical point (τ_{c1}, p_{c1}) and begins at (τ_t, p_t). Meanwhile, there exhibits an IBH/SBH line of coexistence states that terminates at (τ_z, p_z) and begins at (τ_t, p_t). Especially, a "triple point" between the SBH, IBH and LBH appears in the point (τ_t, p_t). We plot the $p - \tau$ diagrams for different γ in the right one of Fig. 9, it is shown that the values of critical points in $p - \tau$ diagrams, i.e. (τ_{c1}, p_{c1}), (τ_t, p_t) and (τ_z, p_z) increases as γ increases.

4.4 Unexpected RPT when $\gamma_T < \gamma \leq \gamma_P$

When $\gamma_T < \gamma \leq \gamma_P$, there exists a single physical critical point, while another positive critical horizon radius corresponds to zero/negative pressure and positive critical temperature, thus physically unobservable. Usually, a single critical point will indicate the first order SBH/LBH phase transition as presented in Sect. 4.2, while two critical points correspond to the RPT as shown in Sect. 4.3. However, when

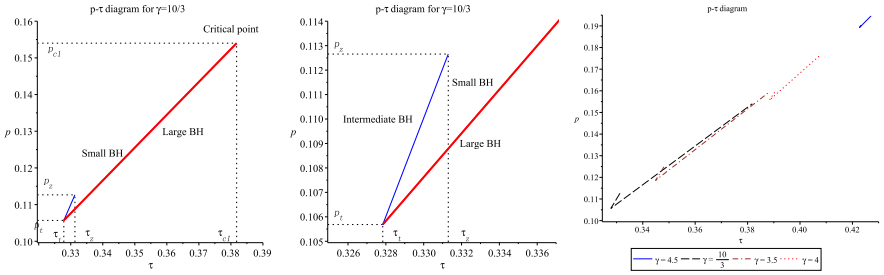

Fig. 8 $p-\tau$ diagram for RPT when $\gamma_P < \gamma < \gamma_m$. The first order SBH/LBH phase transition is depicted by a thick solid line, while the zero oder IBH/SBH phase transition is denoted as the solid line. In the right one, the values of γ for $p-\tau$ curves increases from the left to right

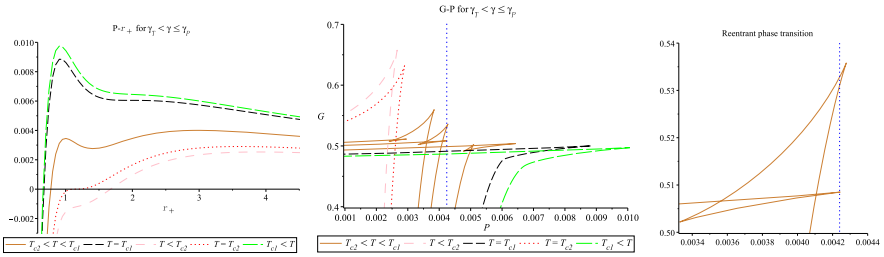

Fig. 9 Curves of $P-r_+$ and $G-P$ for the cases with $\gamma_T < \gamma \leq \gamma_P$. There exists an unexpected RPT. In $P-r_+$ plot, the temperature of isotherms decrease from left to right, while they increase from left to right in $G-P$ plot

$\gamma_T < \gamma \leq \gamma_P$, it will be interesting to observe an unexpected RPT with a single physical critical point for the first time.

The $P-r_+$ and $G-P$ diagrams are depicted in Fig. 9. One can also find two $P-r_+$ oscillatory behavior and multi-characteristic "swallow tail" behavior for the isotherms with temperature $0 < T < T_{c2}$ (as $T_{c1} < 0$) denoted as the (gold) solid line. Similarly to the case in last Sect. 4.3, a RPT can occur, which comprises of a first order SBH/LBH phase transition arising in the range of temperatures $T \in (T_t, T_{c1})$, and a "zero order" IBH/SBH phase transition happening in the range of temperatures $T \in (T_t, T_z)$. Now we consider the coexistence states to explain this unexpected RPT with a single physical critical point. When $\gamma_T < \gamma \leq \gamma_P$, we can find $R_1 > R_m > R_P > R_2 > R_T > R_0$ from Fig. 1. Thus Eq. (30) indicates as well that a phase transition (at least two "swallow tail") should occur when $T_{c2} < T < T_{c1}$. Therefore, one can expect that there should exist an unexpected RPT. Since T_{c2} corresponds to a vanishing or negative pressure P_{c2}, the pressure of the theoretical critical RPT point may be negative. As an effect of the physically unobservable critical point (T_{c2}, P_{c2}), the range of this RPT temperatures $T \in (T_t, T_z)$ may be smaller than the theoretical one, comparing with the normal RPT case in last Sect. 4.3.

We follow the same procedure, i.e. Eqs. (31), (32) and (33) to calculate the theoretical critical RPT points (τ_t, p_t) and (τ_z, p_z) for the cases with $\gamma_T < \gamma \leq \gamma_P$. They are list in Table 3. Even there is a single critical point (τ_{c1}, p_{c1}), as p_{c2} are always negative,

Table 3 The critical points and the theoretical critical RPT points (τ_t, p_t) and (τ_z, p_z) in triple phase diagram when $\gamma_T < \gamma \leq \gamma_P$. For $\gamma = \frac{12}{5}$ and $\frac{5}{2}$, p_z both become negative and could not be physically observed

γ	(τ_{c2}, p_{c2})	(τ_{c1}, p_{c1})	(τ_z, p_z)	(τ_t, p_t)
3	(0.213914, − 0.069404)	(0.368603, 0.143292)	(0.292263, 0.086975)	(0.288595, 0.079275)
2.8	(0.165561, − 0.131049)	(0.360467, 0.136897)	(0.264673, 0.070810)	(0.261041, 0.063379)
2.75	(0.152231, − 0.148117)	(0.358400, 0.135298)	(0.256045, 0.064783)	(0.253589, 0.059442)
2.5	(0.076657, − 0.245371)	(0.347824, 0.127282)	(0.206684, − 0.022839)	(0.212307, 0.040243)
2.4	(0.041572, − 0.290762)	(0.343466, 0.124056)	(0.134922, − 0.098192)	(0.193619, 0.032950)

the critical RPT points (τ_t, p_t) and (τ_z, p_z) could be physical with positive temperature and pressure, e.g. the cases with $\gamma = 3, \frac{14}{5}, \frac{11}{4}$. This novel RPT can be also seen in the $p - \tau$ diagrams (i.e. $P - T$ diagrams) as shown in the left one of Fig. 10. However, when γ continues to decrease, the theoretical critical pressure p_z of the RPT may be negative, e.g. the cases with $\gamma = \frac{12}{5}, \frac{5}{2}$ (See Table 3 and the right one of Fig. 10). We choose $\gamma = \frac{12}{5}$ as an example shown in Fig. 11. In the left one of Fig. 11, it is easy to find that these is no qualitative change for the first order SBH/LBH phase transition beginning at (τ_t, p_t) and ending in (τ_{c1}, p_{c1}); and the "triple point" (τ_t, p_t) between the SBH, IBH and LBH. For the "zero" order IBH/SBH phase transition, it seems to begin at a physically unobservable point (τ_z, p_z) (i.e. $(0.134922, -0.098192)$) and ending in (τ_t, p_t). Actually, the physical beginning of the "zero" order IBH/SBH phase transition should be $(\tau_0, 0)$, which is denoted in the right one of Fig. 11. τ_0 could be directly derived by choosing $p_z = 0$ in Eq. (32), namely

$$\frac{\partial p}{\partial R}|_{(\tau=\tau_z, R=R_a)} = \frac{\partial p}{\partial R}|_{(\tau=\tau_z, R=R_b)} = 0, \quad p_a = p_b = 0. \tag{34}$$

For $\gamma = \frac{12}{5}$ and $\frac{5}{2}$, $\tau_0 \approx 0.179081$ and 0.194280, respectively (See the left one of Fig. 12). For other cases with theoretical critical pressure of RPT $p_z < 0$, τ_0 of the physical critical RPT for different γ are shown in the right one of Fig. 12.

5 Conclusion

In this paper, we present the critical phenomena and phase structure of the Hayward-AdS black hole. The phase structure are very complicated, as there exist not only the liquid/gas like phase transition between LBH and SBH, but also the RPT between the LBH, IBH and SBH. The number of critical points and the types of phase transition depend on the values of γ (i.e. the strength constant α of the nonlinear electrodynamics), which are summarized in the Table 4. It is interesting to find an unexpected RPT with a single physical critical point for the first time, while usually the RPT should correspond to two physical critical points. Besides, the relation $\frac{P_c v_c}{T_c}$ is always a universal constant for different γ, which are slightly different from the value $\frac{3}{8}$ of the van der Waals fluid. We also derive the critical exponents and the coexistence states. For

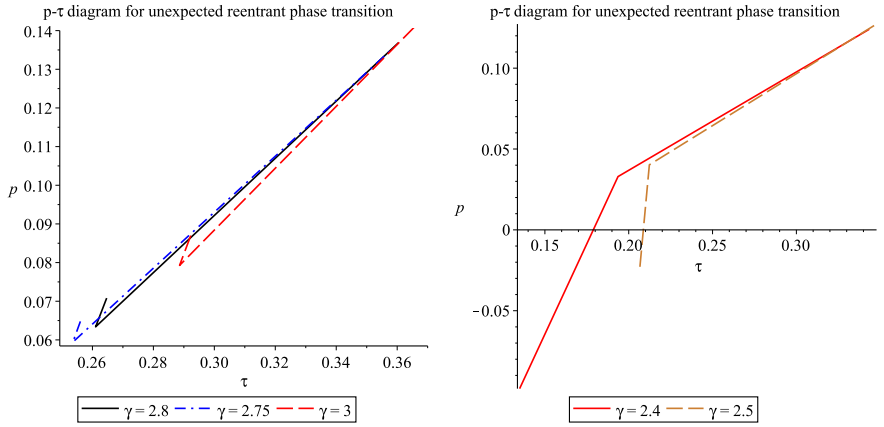

Fig. 10 Theoretical $p - \tau$ diagram for unexpected RPT when $\gamma_T < \gamma \leq \gamma_P$. In the both plots, the values of γ for $p - \tau$ curves increases from the left to right

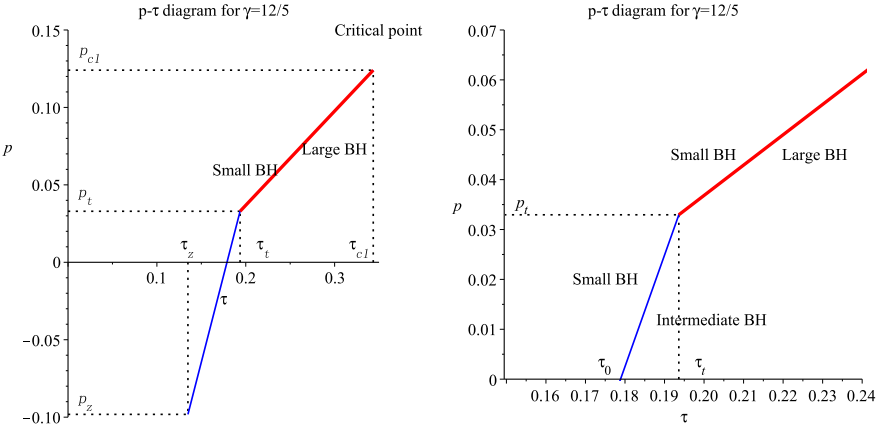

Fig. 11 Theoretical and physical $p - \tau$ diagram for unexpected RPT with $\gamma = \frac{12}{5}$. As $p_z < 0$, the physical beginning of the "zero" order IBH/SBH phase transition should be $(\tau_0, 0)$

the RPT, it comprises of a first order SBH/LBH phase transition beginning at (T_t, P_t) and ending in (T_{c1}, P_{c1}), and a "zero" order IBH/SBH phase transition beginning at (T_z, P_z) and ending in (T_t, P_t). We have presented the way obtaining the critical RPT points (T_z, P_z) and (T_t, P_t), and given their exact values. Especially for the unexpected RPT, if P_z becomes negative, the physical beginning of the "zero" order IBH/SBH phase transition should be $(T_0, 0)$, which is also derived.

It is interesting to find this unexpected RPT with a single critical point in other AdS black hole background, e.g. the Born-Infeld AdS black hole, Gauss-Bonnet AdS black holes, LoveLock AdS black holes and massive AdS black holes, even the Kerr and other rotating AdS black holes, etc. Besides, it would be of great importance to explore the existence of the RPT with a single critical point beyond the black hole

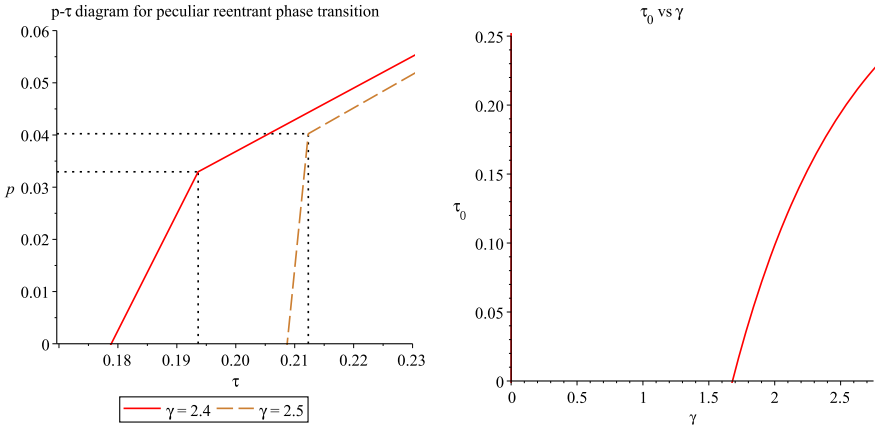

Fig. 12 The left plot is the physical $p - \tau$ diagram for unexpected RPT with $\gamma = \frac{12}{5}$ and $\frac{5}{2}$. If $p_z < 0$, the physical beginning of the "zero" order IBH/SBH phase transition should be $(\tau_0, 0)$, where $\tau_0 = 0.179081$ and 0.194280 for $\gamma = \frac{12}{5}$ and $\frac{5}{2}$, respectively. For other cases with theoretical $p_z < 0$, physical τ_0 for different γ are shown in the right plot

Table 4 The behaviors of critical points and phase transition for different values of γ (or α). The values of special γ are $\gamma_m \approx 4.83$, $\gamma_P \approx 3.27$, $\gamma_T \approx 2.29$

γ	$\gamma \leq \gamma_T$	$\gamma_T < \gamma \leq \gamma_P$	$\gamma_P < \gamma < \gamma_m$	$\gamma = \gamma_m$	$\gamma > \gamma_m$
Number of critical points	1	1	2	1	0
Types of phase transition	First order	Reentrant	Reentrant	No	No

system, namely the quantum multi-body system with interaction, e.g. nicotine/water mixture [20], granular superconductors, liquid crystals, binary gases, ferroelectrics and gels [21], etc. These are all left as the future tasks.

Acknowledgements We are grateful to the anonymous referees for useful suggestions and comments which considerably improved the quality of the manuscript. We would like to thank Bin Zhu and Yuan-Zhang Cui for useful conversations. Wei Xu was supported by the National Natural Science Foundation of China (NSFC) Under Grant Nos. 11505065, 11374330 and 91636111, and the Fundamental Research Funds for the Central Universities, China University of Geosciences (Wuhan).

References

1. Hawking, S.W., Page, D.N.: Thermodynamics of Black Holes in anti-De Sitter Space. Commun. Math. Phys. **87**, 577 (1983)
2. Witten, E.: Anti-de Sitter space, thermal phase transition, and confinement in gauge theories. Adv. Theor. Math. Phys. **2**, 505 (1998). [arXiv:hep-th/9803131]
3. Maldacena, J. M.: The Large N limit of superconformal field theories and supergravity. Int. J. Theor. Phys. **38**, 1113 (1999) [Adv. Theor. Math. Phys. **2**, 231 (1998)]. [arXiv:hep-th/9711200]
4. Gubser, S.S., Klebanov, I.R., Polyakov, A.M.: Gauge theory correlators from noncritical string theory. Phys. Lett. B **428**, 105 (1998)

5. Witten, E.: Anti-de Sitter space and holography. Adv. Theor. Math. Phys. **2**, 253 (1998). [arXiv:hep-th/9802150]
6. Chamblin, A., Emparan, R., Johnson, C.V., Myers, R.C.: Charged AdS black holes and catastrophic holography. Phys. Rev. D **60**, 064018 (1999). [arXiv:hep-th/9902170]
7. Chamblin, A., Emparan, R., Johnson, C.V., Myers, R.C.: Holography, thermodynamics and fluctuations of charged AdS black holes. Phys. Rev. D **60**, 104026 (1999). [arXiv:hep-th/9904197]
8. Dolan, B.P.: Pressure and volume in the first law of black hole thermodynamics. Class. Quant. Grav. **28**, 235017 (2011). [arXiv:1106.6260 [gr-qc]]
9. Cvetic, M., Gibbons, G.W., Kubiznak, D., Pope, C.N.: Black hole enthalpy and an entropy inequality for the thermodynamic volume. Phys. Rev. D **84**, 024037 (2011). [arXiv:1012.2888 [hep-th]]
10. Castro, A., Dehmami, N., Giribet, G., Kastor, D.: On the universality of inner black hole mechanics and higher curvature gravity. JHEP **1307**, 164 (2013). [arXiv:1304.1696 [hep-th]]
11. Dolan, B.P., Kastor, D., Kubiznak, D., Mann, R.B., Traschen, J.: Thermodynamic volumes and isoperimetric inequalities for de sitter black holes. Phys. Rev. D **87**(10), 104017 (2013). [arXiv:1301.5926 [hep-th]]
12. Kastor, D., Ray, S., Traschen, J.: Smarr formula and an extended first law for lovelock gravity. Class. Quant. Grav. **27**, 235014 (2010). [arXiv:1005.5053 [hep-th]]
13. Mahmoud El-Menoufi, B., Ett, B., Kastor, D., Traschen, J.: Gravitational tension and thermodynamics of planar AdS spacetimes. Class. Quant. Grav. **30**, 155003–2435 (2013). [arXiv:1302.6980 [hep-th]]
14. Kubiznak, D., Mann, R.B.: P-V criticality of charged AdS black holes. JHEP **1207**, 033 (2012). [arXiv:1205.0559 [hep-th]]
15. Altamirano, N., Kubiznak, D., Mann, R.B., Sherkatghanad, Z.: Thermodynamics of rotating black holes and black rings: phase transitions and thermodynamic volume. Galaxies **2**, 89 (2014). [arXiv:1401.2586 [hep-th]]
16. Kubiznak, D., Mann, R.B., Teo, M.: Black hole chemistry: thermodynamics with Lambda. Class. Quant. Grav. **34**(6), 063001 (2017). [arXiv:1608.06147 [hep-th]]
17. Gunasekaran, S., Mann, R.B., Kubiznak, D.: Extended phase space thermodynamics for charged and rotating black holes and Born-Infeld vacuum polarization. JHEP **1211**, 110 (2012). [arXiv:1208.6251 [hep-th]]
18. Altamirano, N., Kubiznak, D., Mann, R.B.: Reentrant phase transitions in rotating antiCde Sitter black holes. Phys. Rev. D **88**(10), 101502 (2013). [arXiv:1306.5756 [hep-th]]
19. Hennigar, R.A., Mann, R.B., Tjoa, E.: Superfluid black holes. Phys. Rev. Lett. **118**(2), 021301 (2017). [arXiv:1609.02564 [hep-th]]
20. Hudson, C.: Die gegenseitige lslichkeit von nikotin in wasser. Z. Phys. Chem. **47**, 113 (1904)
21. Narayanan, T., Kumar, A.: Reentrant phase transitions in multicomponent liquid mixtures. Phys. Rep. **249**, 135 (1994)
22. Maslov, V.P.: Zeroth-order phase transitions. Math. Notes **76**, 697 (2004)
23. Frassino, A.M., Kubiznak, D., Mann, R.B., Simovic, F.: Multiple reentrant phase transitions and triple points in lovelock thermodynamics. JHEP **1409**, 080 (2014). [arXiv:1406.7015 [hep-th]]
24. Sherkatghanad, Z., Mirza, B., Mirzaiyan, Z., Hosseini Mansoori, S.A.: Critical behaviors and phase transitions of black holes in higher order gravities and extended phase spaces. Int. J. Mod. Phys. D **26**(03), 1750017 (2016). [arXiv:1412.5028 [gr-qc]]
25. Hennigar, R.A., Brenna, W.G., Mann, R.B.: $P - v$ criticality in quasitopological gravity. JHEP **1507**, 077 (2015). [arXiv:1505.05517 [hep-th]]
26. Kubiznak, D., Simovic, F.: Thermodynamics of horizons: de Sitter black holes and reentrant phase transitions. Class. Quant. Grav. **33**(24), 245001 (2016). [arXiv:1507.08630 [hep-th]]
27. Hennigar, R.A., Mann, R.B.: Reentrant phase transitions and van der Waals behaviour for hairy black holes. Entropy **17**(12), 8056 (2015). [arXiv:1509.06798 [hep-th]]
28. Zou, D.C., Yue, R., Zhang, M.: Reentrant phase transitions of higher-dimensional AdS black holes in dRGT massive gravity. Eur. Phys. J. C **77**(4), 256 (2017). [arXiv:1612.08056 [gr-qc]]
29. Zhang, M., Zou, D.C., Yue, R.H.: Reentrant phase transitions and triple points of topological AdS black holes in Born-Infeld-massive gravity. Adv. High Energy Phys. **2017**, 3819246 (2017). [arXiv:1707.04101 [hep-th]]
30. Hendi, S.H., Momennia, M.: Reentrant phase transition of BornCInfeld-dilaton black holes. Eur. Phys. J. C **78**(10), 800 (2018). [arXiv:1709.09039 [gr-qc]]
31. Dehyadegari, A., Sheykhi, A.: Reentrant phase transition of Born-Infeld-AdS black holes. Phys. Rev. D **98**(2), 024011 (2018). [arXiv:1711.01151 [gr-qc]]

32. Xu, W., Wang, Cy., Zhu, B.: Effects of Gauss-Bonnet term on the phase transition of a Reissner-Nordstrom-AdS black hole in (3+1) dimensions. Phys. Rev. D **99**(4), 044010 (2019)
33. Kord Zangeneh, M., Dehyadegari, A., Sheykhi, A., Mann, R.B.: Microscopic origin of black hole reentrant phase transitions. Phys. Rev. D **97**(8), 084054 (2018). [arXiv:1709.04432 [hep-th]]
34. Born, M., Infeld, L.: Foundations of the new field theory. Proc. Roy. Soc. Lond. A **144**, no. 852, 425 (1934) [J. Phys. Soc. Jap. **8**, no. 8, 307 (1934)]
35. Fradkin, E.S., Tseytlin, A.A.: Nonlinear electrodynamics from quantized strings. Phys. Lett. B **163**, 123–130 (1985)
36. Ayon-Beato, E., Garcia, A.: Regular black hole in general relativity coupled to nonlinear electrodynamics. Phys. Rev. Lett. **80**, 5056 (1998)
37. Ayon-Beato, E., Garcia, A.: New regular black hole solution from nonlinear electrodynamics. Phys. Lett. B **464**, 25 (1999)
38. Hayward, S.A.: Formation and evaporation of regular black holes. Phys. Rev. Lett. **96**, 031103 (2006). [arXiv:gr-qc/0506126]
39. Fan, Z.Y.: Critical phenomena of regular black holes in anti-de Sitter space-time. Eur. Phys. J. C **77**(4), 266 (2017). [arXiv:1609.04489 [hep-th]]
40. Fan, Z.Y., Wang, X.: Construction of regular black holes in general relativity. Phys. Rev. D **94**(12), 124027 (2016). [arXiv:1610.02636 [gr-qc]]
41. Bronnikov, K.A.: Regular magnetic black holes and monopoles from nonlinear electrodynamics. Phys. Rev. D **63**, 044005 (2001)
42. Hassaine, M., Martinez, C.: Higher-dimensional charged black holes solutions with a nonlinear electrodynamics source. Class. Quant. Grav. **25**, 195023 (2008)
43. Balart, L., Vagenas, E.C.: Regular black holes with a nonlinear electrodynamics source. Phys. Rev. D **90**(12), 124045 (2014)
44. Olmo, G.J., Rubiera-Garcia, D.: Palatini $f(R)$ black holes in nonlinear electrodynamics. Phys. Rev. D **84**, 124059 (2011)
45. Hollenstein, L., Lobo, F.S.N.: Exact solutions of f(R) gravity coupled to nonlinear electrodynamics. Phys. Rev. D **78**, 124007 (2008)
46. Ma, M.S.: Magnetically charged regular black hole in a model of nonlinear electrodynamics. Ann. Phys. **362**, 529–537 (2015)
47. Liu, Y., Gong, Y., Wang, B.: Non-equilibrium condensation process in holographic superconductor with nonlinear electrodynamics. JHEP **02**, 116 (2016)
48. He, Y., Ma, M.S.: $(2+1)$-dimensional regular black holes with nonlinear electrodynamics sources. Phys. Lett. B **774**, 229–234 (2017)
49. Zhang, C.Y., Wu, Y.B., Zhang, Y.N., Wang, H.Y., Wu, M.M.: Holographic paramagnetism-ferromagnetism phase transition with the nonlinear electrodynamics. Nucl. Phys. B **914**, 446–460 (2017)
50. Yao, W., Yang, C., Jing, J.: Holographic insulator/superconductor transition with exponential nonlinear electrodynamics probed by entanglement entropy. Eur. Phys. J. C **78**(5), 353 (2018)
51. Breton, N.: Smarrs formula for black holes with non-linear electrodynamics. Gen. Rel. Grav. **37**, 643–650 (2005)
52. Hendi, S.H., Panahiyan, S., Eslam Panah, B.: P-V criticality and geometrical thermodynamics of black holes with Born-Infeld type nonlinear electrodynamics. Int. J. Mod. Phys. D **25**(01), 1650010 (2015)
53. Miskovic, O., Olea, R.: Conserved charges for black holes in Einstein-Gauss-Bonnet gravity coupled to nonlinear electrodynamics in AdS space. Phys. Rev. D **83**, 024011 (2011)
54. Gonzalez, H.A., Hassaine, M., Martinez, C.: Thermodynamics of charged black holes with a nonlinear electrodynamics source. Phys. Rev. D **80**, 104008 (2009)
55. Wang, P., Wu, H., Yang, H.: Thermodynamics of nonlinear electrodynamics black holes and the validity of weak cosmic censorship at charged particle absorption. Eur. Phys. J. C **79**(7), 572 (2019)
56. Dehghani, M.: Thermodynamic properties of dilaton black holes with nonlinear electrodynamics. Phys. Rev. D **98**(4), 044008 (2018)
57. Han, Y.W., Lan, M.J., Zeng, X.X.: Thermodynamics and weak cosmic censorship conjecture in (2+1)-dimensional regular black hole with nonlinear electrodynamics sources. Eur. Phys. J. Plus **135**(2), 172 (2020)
58. Wang, P., Wu, H., Yang, H.: Thermodynamics and phase transition of a nonlinear electrodynamics black hole in a cavity. JHEP **07**, 002 (2019)

59. Kuang, X.M., Liu, B., Övgün, A.: Nonlinear electrodynamics AdS black hole and related phenomena in the extended thermodynamics. Eur. Phys. J. C **78**(10), 840 (2018)
60. Wang, P., Wu, H., Yang, H.: Thermodynamics and phase transitions of nonlinear electrodynamics black holes in an extended phase space. JCAP **04**, 052 (2019)